Reactive current injection protocol for low-power rating distributed generation sources under voltage sags

Jaume Miret, Antonio Camacho, Miguel Castilla, José Luís García de Vicuña, Jordi de la Hoz

Department of Electronic Engineering, UPC, Spain

jmiret@eel.upc.edu

Abstract: Voltage sags are one of the main problems in transmission and distribution networks. This paper proposes a voltage support control scheme for grid-connected low-power rating inverters under voltage sags. Voltage support capability is provided thanks to reactive current injection. The main objective is to inject the maximum rated reactive current during the voltage sag. And second, to raise the higher phase voltage to a predefined maximum boundary, thus preventing over-voltage. Moreover, with this strategy the phase voltages can be equalized. The first objective can be always accomplished during voltage sags. Achieving the second objective depends on the grid characteristics, the sag profile and the power rating of the inverter. Selected experimental results are reported in order to validate the effectiveness of the proposed control.

1 Introduction

The number of renewable energy sources connected to the public grid is significantly increasing due to the deregulation of the electric market and to environmental issues [1]. In this scenario, grid codes have assumed that the contribution of the distributed generation sources (DGS) to the total electric generation was low, but the number of grid-connected DGS is rising year by year. Currently, the transmission system voltage quality is supported by synchronous generators in conventional high-rated power plants and by hardware compensators along the grid [2]. However, during electrical disturbances distributed generation can lead to worsen the stability of the network.

One of the most challenging disturbances is the transitory reduction of the rms voltage in one or more phases, known as voltage sag [3]–[7]. There exists some international standards [8] and national grid codes [9], [10] that regulate the operation of grid-connected DGS under nominal and disturbed conditions. The basic grid code requirements force DGS to act as mere voltage trackers and define the voltage limits measured at the point of common coupling (PCC), known as low-voltage ride-through (LVRT). When the PCC voltage amplitudes are outside these limits, and following a predefined time/sag-depth profile, the DGS must be disconnected. Present grid codes also demand some amount of reactive power injection which helps to support the PCC voltage during voltage sags [9]. The strategy for reactive current injection greatly varies depending on the national grid codes [9]. Clearly, the growing number of DGS connected to the grid will force to new requirements in grid codes [10], [11].

In recent works, flexible injection of reactive power has been used to provide additional functionalities to the DGS [12]–[17]. Some studies, [12]–[14], deal with the mitigation of dc-link voltage oscillations due to grid imbalances. Reference [15] devises a controller which achieves symmetrical grid currents to avoid current harmonic distortion. Reference [16] proposes a controller that ensures minimum peak values in the grid-injected currents. In [17] a dual sequence power injection scheme is proposed to fulfill the LVRT grid code which demands a minimum ratio

between total and reactive current during sags. References [18] to [21] propose different reactive current injection schemes that offer voltage support for mainly inductive grids under voltage sags. In [18] a reference-current generation algorithm that provides flexible voltage support was introduced, although it lacks of any voltage control. Reference [19] presents a voltage control for three-phase inverters based on [18] which requires the measurement of the grid impedance. With this controller the PCC voltages can be restored if the DGS supplies sufficient reactive current. Thus, if the system presents high-power rating, disconnection due to LVRT protocols could be avoided. The limitation of this control scheme is that it can be employed only with types I, II and III sags (also called symmetric sags: equal amplitude drop in one, two or three phases [19]). A significant improvement was done presenting the voltage control scheme for high-power rating DGS reported in [20], which is useful for restoring the PCC voltages to its continuous operation limits under any type of voltage sag. In this way, reference [21] presents a voltage support scheme for static synchronous compensators (STATCOMs) based in PI controllers, thus avoiding the measurement of the grid impedance. In that case a very high power-rating STATCOM is employed for grid-quality improvement, i.e. to confine the PCC voltages between predefined set points near 1 p.u.

In this way, this paper proposes a voltage support controller for low-power rating DGS valid for any type of sag and based on the current scheme introduced in [18]. Ideally, a voltage support control would avoid disconnection due to LVRT protocols. However, in case of deep sags, low-power rating DGS can not restore the PCC voltages to its continuous operation limits, thus less ambitious objectives should be proposed. Moreover due to the growing number of DGS present in the grid, voltage support objectives that can favor distributed operation must be investigated. In this low-power scenario flexible positive and negative reactive power injection can be used to fulfill two new control objectives during sags: first to achieve maximum reactive current injection supporting the lowest amplitude PCC phase voltage as much as possible, and second to set the higher phase

voltage to a predefined upper voltage limit. First objective will be always accomplished, although the second objective could be fulfilled or not depending on grid stiffness and DGS rated power. With this strategy the positive sequence reactive current increases the dropped grid voltages while preventing over-voltage in the higher phase voltage. On the other hand, negative-sequence reactive-power tends to equalize the phase voltages. These two combined objectives will assist the grid stability, also guaranteeing that over-currents flowing through the DGS are avoided and that the maximum voltage boundary is not surpassed in any phase voltage.

The paper is organized as follows. Section 2 describes the grid connected DGS system, analyzes the PCC voltages and the grid code requirements during voltage sags. Section 3 presents the control objectives. Section 4 develops the control proposal. Section 5 corroborates the expected features of the proposed controller by means of selected experimental results. Section 6 presents the conclusions.

2 Grid-connected inverters under voltage sags

This section deals with the description and characterization of the grid-connected DGS under voltage sags. Also the basic grid code requirements during these disturbances are described.

2.1 Grid-connected three-phase inverter

The diagram of a DGS connected to the PCC through a three-phase three-wire inverter and a LCL filter is shown in Fig. 1. When the system is connected to the grid via a mainly inductive line, the mains can be modeled with an inductance L_g, and the source $\mathbf{v_g}$. The controller senses the inverter output current $\mathbf{i}$, and the PCC line-to-line voltages $\mathbf{v}$.

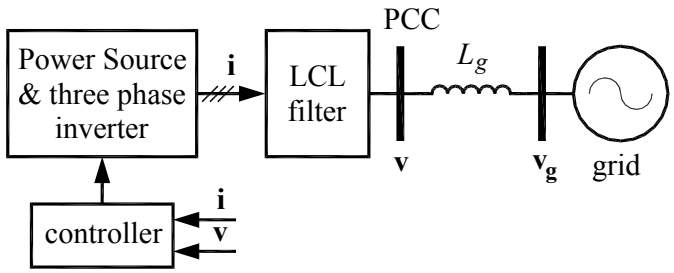

Fig. 1 *Diagram of a grid-connected DGS.*

2.2 Voltage sag characterization

The instantaneous PCC phase voltages during voltage sags can be described as the addition of positive, negative and zero symmetric sequences. Neglecting the initial phase jump and due to the line-to-line monitoring of the voltage sag [4], the instantaneous PCC phase voltages can be expressed in the stationary reference frame (SRF) as

$$v_\alpha = v_{\alpha p} + v_{\alpha n} = V_p \cos(\omega t) + V_n \cos(\omega t + \delta) \tag{1}$$

$$v_\beta = v_{\beta p} + v_{\beta n} = V_p \sin(\omega t) - V_n \sin(\omega t + \delta) \tag{2}$$

where $v_{\alpha p}$, $v_{\beta p}$ and $v_{\alpha n}$, $v_{\beta n}$ are the SRF positive and negative voltage sequences respectively, V_p and V_n are their amplitudes, ω is the grid angular frequency, and δ is the phase angle between positive and negative sequences. The magnitudes V_p, V_n can be determined using the SRF theory [22] and δ can be devised through simple trigonometric manipulations, see [19]. In this case a star-delta-connected transformer is used to interface the DGS to the grid, thus the zero sequence component is zero.

From (1) and (2), the amplitude of the natural frame phase voltages can be written as a function of V_p, V_n and the phase angle δ as

$$V_a = \sqrt{V_p^2 + V_n^2 + 2V_pV_n\cos(\delta)} \tag{3}$$

$$V_b = \sqrt{V_p^2 + V_n^2 + 2V_pV_n\cos(\delta - 2/3\pi)} \tag{4}$$

$$V_c = \sqrt{V_p^2 + V_n^2 + 2V_pV_n\cos(\delta + 2/3\pi)} \tag{5}$$

where V_a, V_b and V_c are the amplitudes of the PCC phase voltages. These amplitudes will be used below to develop the control proposal of this work.

2.3 Grid code requirements under voltage sags

The main objective of a grid connected DGS is to deliver the generated power to the grid. During a voltage sag other objectives are additionally required by grid codes, such as LVRT and reactive current injection. Under the point of view of LVRT protocols, national grid codes and international standards establish the PCC voltage limits for continuous operation. These limits range from a minimum voltage of 0.85 per unit (p.u.) to a maximum value of 1.1 p.u. of the base voltage [8]. When a voltage sag occurs and the minimum limit is under-passed, or the maximum limit is over-passed, by one or more phase voltages, the DGS must be disconnected from the grid after a predefined trip-time.

Additionally, wind grid codes require some amount of reactive current injection during voltage sags in order to support the transmission or distribution system. Although all national grid codes states this injection, they demand different reactive current injection protocols [9].

3 Formulation of objectives and proposed control algorithm

The aim of this section is to define the control objectives and to devise the control algorithm that allows their practical implementation.

An interesting new ancillary functionality of reactive current injection would be to combine maximum current injection and some voltage support capabilities, in order to better sustain the grid

voltage during sags. Additionally, if the active power reference P^* is set to zero during the sag, then all the available power can be dedicated to that purpose.

When an inverter injects reactive power to a mainly inductive grid, the PCC phase voltages will increase proportionally to their phase current amplitudes. Thus, low values of grid impedance produce low voltage increments and then light voltage support. Higher impedance values improve the voltage support capability. Reactive current injection can be done via positive I_p, and/or negative sequences I_n, with different consequences in the PCC voltages [18]. Balancing appropriately the amount of I_p and I_n different protocols can be used to support the grid during the sag.

3.1 Comparison of different voltage support protocols

Fig. 2 shows five examples of voltage support strategies during the same sag in different grid scenarios: with low and high L_g value, with low, high and very high-power rated DGS, and with different reactive current injection protocols (see Table 1).

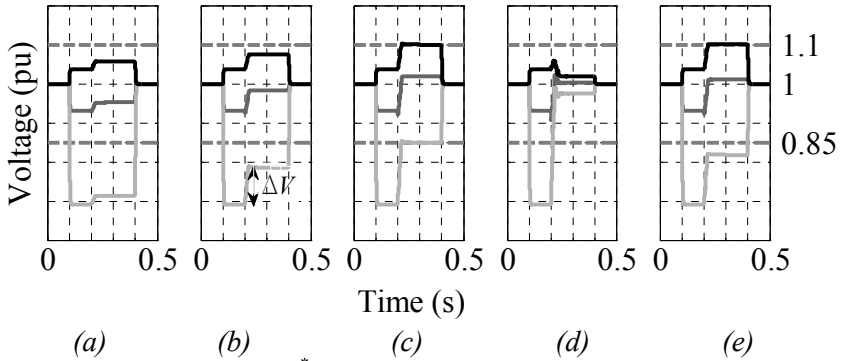

Fig. 2 Voltage support during a sag, with $P^*= 0$ and different reactive injection protocols and scenarios, see Table 1.

Table 1 *Conditions for simulation scenarios in Fig. 2*

	grid inductance	power rating	control protocol	maximum current
a	low	low	$I_p = I_M$ $I_n = 0$	I_M
b	high	low	$I_p > 0$ $I_n > 0$ [20]	I_M
c	high	high	$I_p > 0$ $I_n > 0$ [20]	$1.5I_M$
d	high	very high	$I_p > 0$ $I_n > 0$ $V_{PCC}^* \cong 1$ p.u.	$3I_M$
e	high	low	$I_p > 0$ $I_n > 0$ **proposed**	I_M

Fig. 2 (a) shows the PCC phase voltage amplitudes during a voltage sag in a stiff grid (low grid-inductance value). Before t = 0.1 s, the phase voltages are at their nominal amplitude, 1 p.u. At t = 0.1 s, a sag occurs and one phase voltage drops below the minimum operation boundary. Maximum available reactive current injection begins at t = 0.2 s. Note that the reactive injection protocol remains intentionally inactive from t = 0.1 s to t = 0.2 s in order to clearly show the sag profile. In this case only positive sequence current is injected, being zero the negative sequence current,

$$I_p = I_{rated\ current} \tag{6}$$

$$I_n = 0, \tag{7}$$

where $I_{rated\ current}$ is the amplitude of the maximum allowed current. This rated current will be named hereon as maximum allowed current I_M. Consequently the phase current I_a, I_b and I_c are balanced with amplitude I_M. Due to the balanced currents, the voltage increment ΔV is equal in the three phases. Although maximum allowed current is injected, the voltage increment is small due to the low grid-inductance value and the phase with lower amplitude still remains outside the limits for continuous operation.

Fig. 2 (b) shows the sag in a weak grid scenario where the grid inductance value is five times larger than in case (a). In this case the reactive current injection is based on the voltage control presented in [20]. The objectives in that work were: to set the higher PCC phase voltage to 1.1 p.u. and the lower phase voltage to 0.85 p.u.. In the current example, these objectives are not fulfilled due to the low power rating DGS. In [20], when one phase-current reaches the maximum allowed amplitude I_M, the control is saturated in both sequences in order to protect the inverter. Despite to the saturation, the positive-negative sequence current injection provides unbalanced currents, with the highest current of the three phases presenting an amplitude of I_M. It is worth mentioning that the phase voltage with lower amplitude remains outside the limits for continuous operation. If a DGS with higher power-rating was used, the two control objectives could be fulfilled.

Fig. 2 (c) shows the sag in a weak grid scenario but with a higher power-rating DGS. As it can be seen, thanks to the control scheme [20], the PCC voltages are confined between the limits for continuous operation through a higher maximum-current injection, in this case $1.5I_M$. Afterward the voltage support scheme presented in [20] works perfectly in this scenario.

Fig. 2 (d) shows the sag in the same weak grid scenario but in this case a very high power rating inverter is considered (an STATCOM for example, [21]). Also the reactive current injection is done via both sequences but the control objective is to set the PCC voltages roughly to 1 p.u. In this scenario the maximum current presents an amplitude of $3I_M$. Setting the PCC voltages exactly to 1 p.u. would force higher currents due the high negative sequence current I_n required to provide voltage equalization between phases [18], [21].

Fig. 2 (e) shows the sag in the same weak grid scenario than is the last three tests, but assuming a low power rated DGS (maximum allowed current is I_M). As it can be seen in (b), the phase voltage with lower amplitude could not be supported sufficiently to bring the system to continuous operation mode due to the low-power rating of the DGS. Then, in this scenario, instead of the scheme presented in [20], a better voltage support algorithm can be proposed. The new proposal of this work is to set the higher PCC voltage to 1.1 p.u. (avoiding surpassing the upper operation limit as proposed in [20]), and, as a new feature, to provide maximum rising to the most perturbed phase voltage (lower-amplitude one) by maximum current injection. Fig. 2 (e) shows the simulation results of this voltage support protocol. As can be noted in this figure, the main objective of our proposal is not to avoid disconnection due to LVRT protocols. In this scenario avoid disconnection is impossible, no matter the control scheme used, due to the low power rating of the system. On the other hand, as it can be clearly seen by comparing (b) and (e), the proposed solution improves the voltage support in the three phases, without exceeding the maximum current I_M.

Then this proposed scheme is a promising candidate to provide voltage support in low-power rating DGS.

3.2 Proposed voltage support protocol

The new voltage support scheme with results shown in Fig. 2 (e) is based on maximum current injection and phase voltages equalization, and can be summarized in the following objectives:

1) to inject maximum rated current in the most perturbed phase (i.e. phase with lower amplitude), and

2) to avoid exceeding the upper voltage boundary when injecting reactive power.

Examining carefully Fig. 2 (e) it can be noted that ΔV takes a minimum value in the phase with higher voltage amplitude V_M, bringing this phase just to the upper voltage boundary. Of course, this minimum voltage increment will be produced by the minimum amplitude current I_m. On the other hand, ΔV takes a maximum value in the lowest amplitude phase voltage (due to maximum amplitude current I_M), ensuring that the most dropped phase is the most supported. Objectives 1) and 2) are recapitulated in the following equations

$$I_M = I_{rated\ \text{current}} \tag{8}$$

$$V_M = 1.1\ \text{p.u.} \tag{9}$$

where $I_M = \max\{I_a, I_b, I_c\}$ and $V_M = \max\{V_a, V_b, V_c\}$. To achieve (9) minimum current, $I_m = \min\{I_a, I_b, I_c\}$, must be injected in the phase with higher voltage amplitude, V_M. The phase current I_m is related with its phase voltage V_M by a function $\gamma(\cdot)$, which will be determined in next section

$$I_m = \gamma(V_M - 1.1)\ . \tag{10}$$

When the inverter can not afford the required current to accomplish the second objective due its natural physical limitations (i.e. when $I_m > I_M$), then the phase voltages will be below the upper limit and negative sequence current injection has no meaning. The best choice in this case is to inject only positive sequence current, following (6) and (7), since it produces higher ΔV.

Fig. 3 shows the flux diagram of the control algorithm to be implemented.

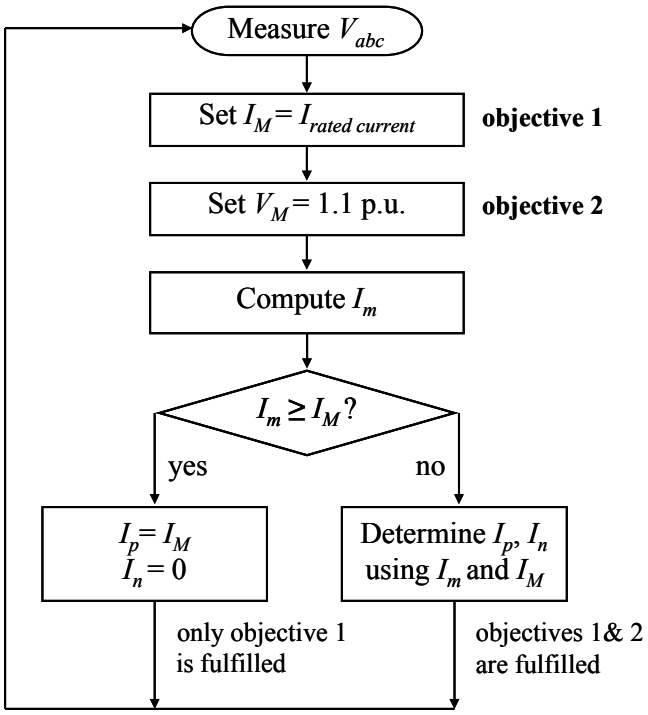

Fig. 3 Flux diagram to determine the support control strategy under different conditions.

First the maximum phase current, I_M, must be set to the maximum rated current. Second, the higher phase voltage must be determined and consequently the minimum phase current, I_m, can be calculated with the aim of raising this voltage to 1.1 p.u. If this minimum phase current is higher than the maximum rated current, the reactive power injection is done only via positive sequence, I_p. On the other hand the reactive power injection is done via both positive and negative sequence currents, I_p and I_n. In next section, the mathematical relationships between phase and sequence variables will be found to develop the expressions to practically implement the control proposal.

4 Theoretical approach to the control scheme

To fulfill the control purposes, first the expression of the PCC natural frame currents during voltage sags will be analyzed, taking into account their positive and negative sequences. After that, their amplitudes will be chosen appropriately to accomplish the objectives expressed in (8)–(9).

4.1 Current injection during voltage sags

According to the instantaneous power theory, the active power, p, and reactive power, q, injected to

the grid by a three phase inverter can be defined as:

$$p = \frac{3}{2}(v_\alpha i_\alpha + v_\beta i_\beta) \tag{11}$$

$$q = \frac{3}{2}(-v_\beta i_\alpha + v_\alpha i_\beta)\,. \tag{12}$$

The reference currents can be derived by ensuring that the instantaneous powers track their references, assuming that the inner current control loop is properly tuned, (i.e. there exists a perfect matching between the reference and the generated current, $\mathbf{i} = \mathbf{i}^*$). After that, the SRF currents can be decomposed in active and reactive current components

$$i_\alpha^* = i_\alpha^*(p) + i_\alpha^*(q) \tag{13}$$

$$i_\beta^* = i_\beta^*(p) + i_\beta^*(q)\,. \tag{14}$$

During voltage sags, if the active power reference is set to zero, all the rated current can be used to support the grid stability, thus improving the functionalities of the DGS. This slight loss of power generation has a minimum impact in the overall efficiency of the system, due to the usual short-time duration of voltage sags. Then, based on [18], the reference reactive/active currents can be defined as

$$i_\alpha^*(q) = \frac{I_p^*}{V_p} v_{\beta p} + \frac{I_n^*}{V_n} v_{\beta n} \tag{15}$$

$$i_\beta^*(q) = -\frac{I_p^*}{V_p} v_{\alpha p} - \frac{I_n^*}{V_n} v_{\alpha n} \tag{16}$$

$$i_\alpha^*(p) = i_\beta^*(p) = 0 \tag{17}$$

where I_p^* and I_n^* are the positive and the negative sequence components of the reactive current references, respectively. It must be noted that it is necessary to find the proper values of I_p^* and I_n^* to perform the chosen control objectives. Therefore, similarly to (3)–(5), the natural frame amplitudes of the phase currents can be expressed as

$$I_a = \sqrt{I_p^{*2} + I_n^{*2} - 2I_p^* I_n^* \cos(\delta)} \tag{18}$$

$$I_b = \sqrt{I_p^{*2} + I_n^{*2} - 2I_p^* I_n^* \cos(\delta - 2/3\,\pi)} \tag{19}$$

$$I_c = \sqrt{I_p^{*2} + I_n^{*2} - 2I_p^* I_n^* \cos(\delta + 2/3\,\pi)}\,. \tag{20}$$

By choosing appropriately I_p^* and I_n^* the values of the minimum and the maximum amplitude phase-currents can be determined, see (8) and (9).

4.2 First objective: maximum current injection

To fulfill the first objective, the expression of the maximum current amplitude must be calculated. From (18)–(20), it can be clearly noted that the minimum and maximum amplitude phase currents are related with the maximum, cos_M, and minimum, cos_m, value of the cosines functions, respectively

$$cos_M = \max\left\{\cos(\delta), \cos(\delta - {}^2/_3\,\pi), \cos(\delta + {}^2/_3\,\pi)\right\} \tag{21}$$

$$cos_m = \min\left\{\cos(\delta), \cos(\delta - {}^2/_3\,\pi), \cos(\delta + {}^2/_3\,\pi)\right\}. \tag{22}$$

Thus the minimum, I_m, and maximum, I_M, amplitude phase currents are

$$I_m = \sqrt{I_p^{*2} + I_n^{*2} - 2I_p^* I_n^* cos_M} \tag{23}$$

$$I_M = \sqrt{I_p^{*2} + I_n^{*2} - 2I_p^* I_n^* cos_m}\,. \tag{24}$$

Note that the reference value for I_M will be set by the designer taking into account the inverter maximum current rating, then accomplishing the first objective. I_m will be determined below to

fulfill the second objective.

4.3 Second objective: to raise the PCC voltages preventing over voltage

The second control objective is to raise the PCC voltages, preventing any phase from surpassing the upper voltage boundary. This objective can be accomplished by first determining the higher amplitude of the grid phase voltages, V_M, and the appropriate minimum-amplitude reactive- current to be injected in order to raise this voltage to 1.1 p.u.

From Fig. 1, the grid voltage can be expressed as

$$\mathbf{v_g} = \mathbf{v} - L_g \frac{\mathrm{d}\mathbf{i}^*(q)}{\mathrm{d}t}. \tag{25}$$

The amplitudes of the positive and negative grid voltage sequences, when injecting a known reactive current, can be derived by inserting (1), (2) and (13)–(17) in (25)

$$V_{gp} = V_p - \omega L_g I_p^* \tag{26}$$

$$V_{gn} = V_n + \omega L_g I_n^*. \tag{27}$$

From (26) and (27), the amplitudes of the grid voltage sequence components can be calculated on-line by assuming that the grid inductance is a known value (a method for measuring L_g on-line can be found in [23]). The higher amplitude of the grid phase voltages, V_{gM}, can be derived using the amplitudes of the grid voltage sequence components (26) and (27) following the previous approach employed for the phase currents (18)–(24)

$$V_{gM} = \sqrt{V_{gp}^2 + V_{gn}^2 + 2V_{gp}V_{gn}\,cos_M}\ . \tag{28}$$

Then, the voltage increment that prevents from exceeding the upper voltage boundary is

$$\Delta V = 1.1 - V_{gM} \tag{29}$$

being this increment produced by the lowest amplitude phase current, I_m, as discussed above,

$$\Delta V = \omega L_g I_m \cos(\theta). \tag{30}$$

The term $\cos(\theta)$ appears due to the phase shift between phase voltage and phase current produced by the simultaneous positive and negative sequence current injection. The angle θ takes the value

$$\theta = tan^{-1}\left(\frac{-V_n\, sin_M}{V_p + V_n\, cos_M}\right) - tan^{-1}\left(\frac{I_n^*\, sin_M}{I_p^* - I_n^*\, cos_M}\right), \tag{31}$$

where sin_M is the sine value of the angle δ, $\delta - 2/3\,\pi$ or $\delta + 2/3\,\pi$, that presents maximum cosine value cos_M.

After that, the reference current value which will raise the higher PCC phase voltage to 1.1 p.u. can be calculated rearranging (30)

$$I_m^* = \frac{\Delta V}{\omega L_g \cos(\theta)}. \tag{32}$$

4.4 Derivation of the control parameters I_p^* and I_n^* under different grid scenarios

Taking the known values of the maximum, (24), and the minimum, (32), phase current amplitudes, the following two equations can be written

$$I_M^* = I_{rated\_current} = \sqrt{I_p^{*2} + I_n^{*2} - 2I_p^* I_n^* cos_m} \tag{33}$$

$$I_m^* = \frac{\Delta V}{\omega L_g\, cos(\theta)} = \sqrt{I_p^{*2} + I_n^{*2} - 2I_p^* I_n^* cos_M}\,. \tag{34}$$

By solving (33) and (34), the values for I_p^* and I_n^* that satisfy the biquadrate system can be found as

$$I_p^* = +\sqrt{\frac{\left(I_M^{*2}\, cos_M - I_m^{*2}\, cos_m\right) + \sqrt{I_M^{*4} x + I_m^{*4} y + 2 I_M^{*2} I_m^{*2} z}}{2\left(cos_M - cos_m\right)}} \tag{35}$$

$$I_n^* = +\sqrt{\frac{\left(I_M^{*2}\, cos_M - I_m^{*2}\, cos_m\right) - \sqrt{I_M^{*4} x + I_m^{*4} y + 2 I_M^{*2} I_m^{*2} z}}{2\left(cos_M - cos_m\right)}}\ , \tag{36}$$

with $x = cos_M{}^2 - 1$, $y = cos_m{}^2 - 1$ and $z = 1 - cos_m\, cos_M$.

When the current amplitude required to raise the higher phase voltage to 1.1 p.u. is lower than the maximum rated current ($I_m{}^* \leq I_M{}^*$), the values obtained in (35) and (36) can be used in the current scheme (15) and (16) and both control objectives are satisfied. Conversely, when $I_m{}^* > I_M{}^*$, only positive sequence current is injected, i.e. $I_p{}^* = I_{rated\ current}$, $I_n{}^* = 0$, see flux diagram of Fig. 3. Depending on the sag profile both references can present values between 0 and $I_{rated\ current}$, with boundary values $I_p{}^* = I_{rated\ curren,}\, I_n{}^* = 0$ and $I_p{}^* = 0,\, I_n{}^* = I_{rated\ current}$. In addition, it must be noted that a high unbalancing between currents can cause overheating in some power switches. This is not desired in normal operation but is not a severe limitation due the usual short duration of the sag.

4.5 Proposed control scheme

The proposed reactive current control scheme is depicted in Fig. 4. In the first block, the voltage at the PCC is sensed and processed on the basis of the SRF theory with the following steps: 1) it detects the voltage sag by comparing the rms values of the PCC voltages with the lower boundary limit; 2) in the case of a voltage sag, it extracts the amplitudes of the voltage sequences, V_p and V_n, and the phase angle δ. The second block is responsible for calculating the amplitudes of the grid voltage sequence components by means of the plant model, which uses the estimated value of the grid impedance and the current references, $I_p{}^*$ and $I_n{}^*$. The third block determines the minimum phase current, $I_m{}^*$, that must be injected to raise the higher PCC voltage to 1.1 p.u. The fourth block computes the sequence current reference amplitudes $I_p{}^*$ and $I_n{}^*$ using the calculated minimum phase current, $I_m{}^*$, and the design parameter which is the rated current, $I_M{}^*$.

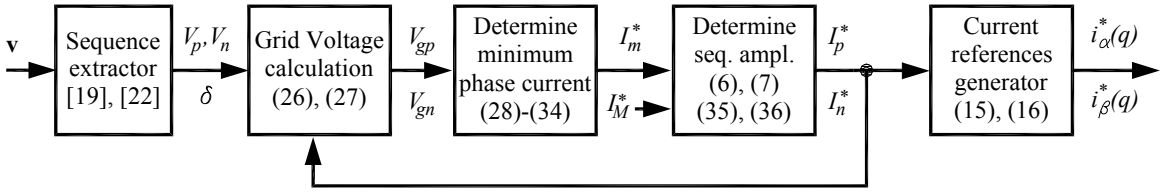

Fig. 4 Block diagram of the proposed voltage support control scheme.

5 Experimental results

An inverter prototype rated at 2.3 kVA was built using a SEMIKRON full-bridge with a resistor damped LCL filter. The DGS behavior is implemented using an AMREL-SPS1000 dc-source. The utility grid is emulated by means of a programmable three-phase Pacific AMX-360 ac-source connected to the PCC with coupling inductors modeling the line inductance. A TMS320F28335 floating point digital signal processor was chosen as the control platform.

A sequence detector implemented with generalized integrators is used to evaluate the voltage vector sequences [22]. The settling time of the sequence detector is 1.5 grid periods due its filter behavior. All the mathematical calculations that implement the controller are done in roughly 40 μs, resulting in a period idle time of 60%. The computed reference-current sequence-components present oscillations at twice the grid frequency, due to system unbalancing. To reduce this noise a low-pass filter with a cut-off frequency below the grid frequency is placed before the current generator block. The current control consists of a proportional-resonant controller [24] and a space vector PWM.

Table 2 lists the parameter values of the inverter and controller. Two different line inductance values (0.06 p.u. and 0.02 p.u.) were used in the test. The higher of them was chosen in the same order of magnitude than the inductance of the LCL filter in order to clearly show the capacity of voltage support provided by the proposed control scheme. Due to the low-power rating of the DGS, smaller values of this inductance would make difficult to appreciate the voltage restoration behavior.

Table 2 *System Parameters*

nominal rated power (base power)	S_b	2.3 kVA
active power reference	P^*	750 W
maximum current amplitude	I_M	10 A
grid voltage line to neutral	V_g	110 V rms
grid frequency	f	60 Hz
dc-link voltage	v_{dc}	350 V
LCL inverter side inductances	L_i	5 mH
LCL filter capacitors	C_o	1.5 μF
LCL resonance damping resistors	R_o	68 Ω
LCL output side inductances	L_o	2 mH
line inductances	L_g	2.5 mH, 0.84 mH
cut-off frequency of the reference current sequences LPF	f_c	40 Hz
proportional gain PRES compensator	k_p	30
integral gain PRES compensator	k_i	50
sampling/switching frequency	f_s	10 kHz

5.1 Voltage sag without support service

A variable-profile voltage sag was programmed in the ac-source to evaluate the behavior of the system, see Fig. 5 (top). The proposed control can deal with any type of voltage sag, although the sag with slow recovery described in [6] is reproduced here due its complex profile: first it presents a type I voltage sag (one dropped phase-voltage), then a second phase begins to drop dynamically (change in δ *from* $^{\pi}/_{3}$ to $^{2\pi}/_{3}$), evolving to a clear type II at the sag-end [4], [19]. To correctly sense the sag, delta connection monitoring was used in this test [4]. The sag follows this sequential behavior: first, during 0.1 seconds, the grid voltages are almost balanced with the following rms voltages: 1.031 p.u., 1.036 p.u. and 1.038 p.u. At time t = 0.1 s, the sag begins and evolves during 0.3 s. At t = 0.4 s the fault is cleared and the PCC voltages recover their pre-fault values. Fig. 5 (middle) shows the rms values of the PCC phase voltages during the voltage sag. A dashed line at 1.1 p.u. is drawn horizontally to highlight the chosen upper voltage boundary. Fig. 5 (bottom) shows the measured positive and negative voltage sequences.

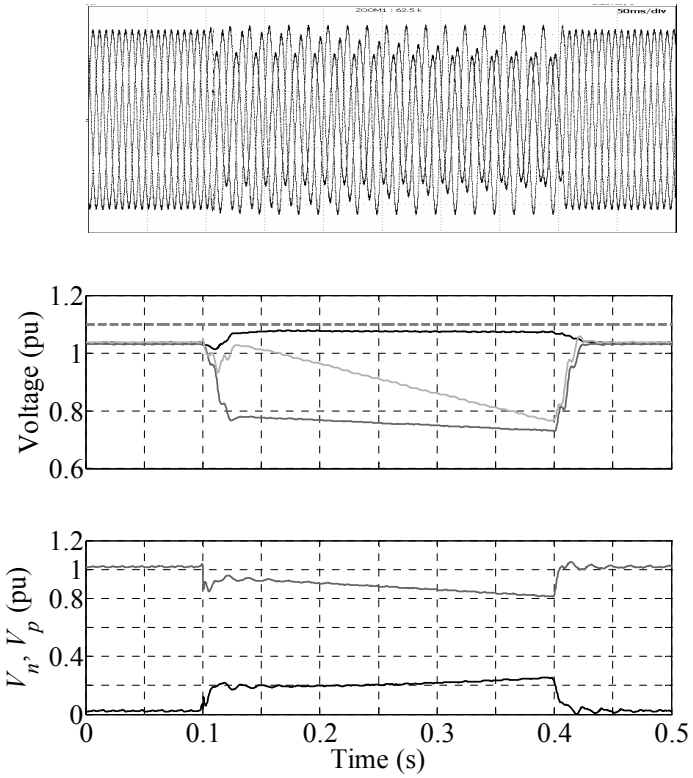

Fig. 5 Measured PCC voltages. Top: phase voltages (50 V/div.). Middle: rms phase voltages. Bottom: amplitudes of the positive (in gray) and negative (in black) voltage sequence components. Test without activation of the proposed control.

5.2 Supporting sags in a stiff grid

To demonstrate the proposed control behavior, the support control kicks in at t = 0.1 s and, after one grid cycle necessary to stabilize the voltage measurements, the correction begins. In this first experiment, a stiff grid is supposed, thus an L_g = 0.84 mH is used to emulate the line impedance (corresponding to 0.02 p.u.).

Fig. 6 (top) shows the injected currents when the control is activated. Before the sag, the inverter is injecting an active power of P^* = 750 W. When the sag is detected the active power injection ceases, P^* = 0, and only reactive current is injected. Due to the stiffness of the grid, the second objective (raising the higher PCC voltage amplitude to 1.1 p.u.) can not be fulfilled. This issue is detected by the controller and thus all the reactive current is injected only via positive sequence (I_p^* = 10 A, I_n^* = 0 A). Thus the phase currents are perfectly balanced and only the first control objective (I_M = 10 A) is satisfied.

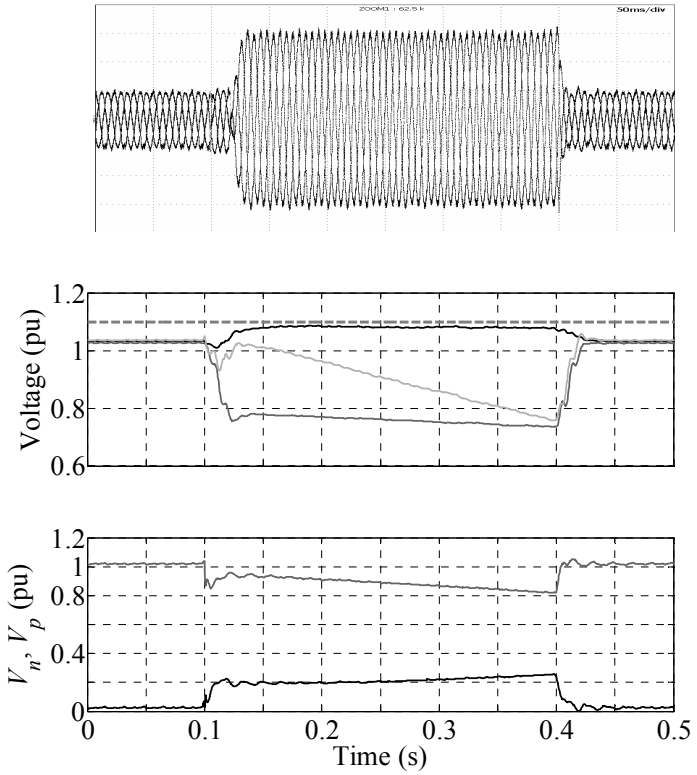

Fig. 6 Measured PCC currents and voltages. Top: inverter phase currents (3.3 A/div.). Middle: rms phase voltages. Bottom: positive (in gray) and negative (in black) voltage sequence components. Proposed control activated, supporting a stiff grid, $L_g = 0.02$ p.u.

Fig. 6 (midle) shows the PCC phase voltages during the experiment. Comparing this figure with Fig. 5 (middle), it can be observed that all the phase voltages rise slightly. Only a precise comparison between Fig. 5 and Fig. 6 confirms this small voltage raise.

The second objective is not satisfied, as the higher amplitude PCC voltage is raised but placed below 1.1 p.u. Since only positive current injection is done, only the positive sequence voltage amplitude is affected, being the negative sequence voltage amplitude unaltered, see Fig. 6 (bottom). In this test the minimum current necessary to raise the phase voltage to 1.1 p.u. is $I_m^* \approx 20$ A. It must be noted that this high current amplitude is required due to the grid stiffness. This current is higher than the inverter rated current (10 A) and the second objective can not be fulfilled. The controller detects this issue and sets the current references according to the algorithm shown in Fig. 3. It must be noted that, during the sag, the system becomes unbalanced, and an oscillation at twice the line frequency appears in both active and reactive power.

5.3 Supporting sags in a weak grid

When supporting a weak grid, i.e., remote sag locations with high line inductance, the PCC voltage amplitudes can be raised with less reactive power injection than in a stiff grid scenario. In this second experiment a higher line inductance value was used, L_g = 2.5 mH (0.06 p.u.).

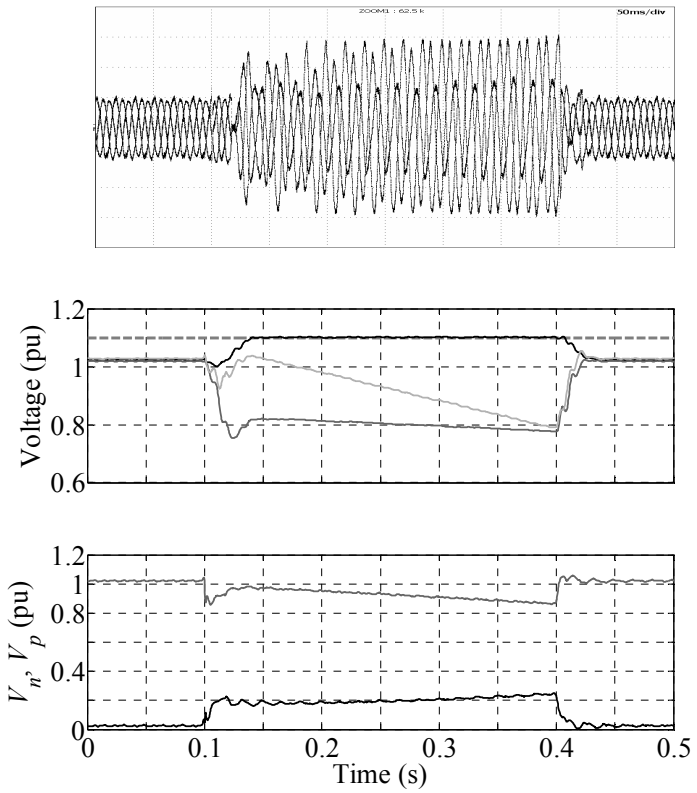

Fig. 7 Measured PCC currents and voltages. Top: inverter phase currents (3.3 A/div.). Middle: rms phase voltages. Bottom: amplitudes of the positive (in gray) and negative (in black) voltage sequence components. Proposed control activated, supporting a weak grid, L_g = 0.06 p.u.

Fig. 7 (top) shows the injected currents when supporting a weak grid. The first control objective, to set at least one phase current at its maximum rated value, I_M = 10 A, is also accomplished after a settling time of 70 ms. In this experiment the reactive current is injected via positive and negative sequences (I_p^* > 0 and I_n^* > 0 A), thus unbalancing the phase currents. Fig. 7 (middle) shows the rms values of the PCC phase voltages during the supported voltage sag. It can be observed that the higher voltage raises to 1.1 p.u., satisfying the second control objective. Comparing the positive and negative sequence amplitudes (bottom) with the respective graphs shown in Fig. 5 (voltage sag without support), it can be noted an increment in the positive sequence

and a decrement in the negative sequence.

In all the previous tests, and also in this last experiment, and due to the low power rating of the DGS, the disconnection of the system due to LVRT protocols has not been avoided. In real transmission systems only high-power rating DGS (or STATCOMS) are capable of fulfill a successful voltage support that would avoid disconnection.

5.4 Supporting different kinds of voltage sags

A complete set of simulations has been done with the intention of demonstrate the effectiveness of the proposal under any kind of voltage sag. The system with parameters described in Table 2 has been simulated under weak grid scenario. In this simulation a more realistic grid-impedance with an R/X ratio of 0.25 has been tested. Six sags characterized by its common parameters: V_p = 0.82 p.u., V_n = 0.2 p.u. and a sequence phase angle with different values $\delta = n \cdot {}^{\pi}/_{8}$ rad. (for n = 0 to n = 7), have been implemented in order to obtain a wide range of sag-types [4], [19]. Fig. 8 shows the PCC phase voltages during these different sags. The sag begins at t = 0.1 s., and the control is activated at t = 0.2 s. When $\delta = 0$ an almost pure type II sag is simulated. On the other cases nonsymmetrical sags are produced. In all the tests the most perturbed phase is the most supported (objective 1: injected reactive current equal to I_M). And the higher phase voltage never surpasses 1.1. p.u. (objective 2). The slight difference between the two drooped phases in type II case ($\delta = 0$) is due the presence of resistive behavior in the grid-impedance (R/X=0.25). This difference is also present in the other test but is difficult to appreciate. Table 3 presents the amplitudes of the sequence and phase currents in these simulations. As in previous tests LVRT disconnection is not avoided due to the low-power rating.

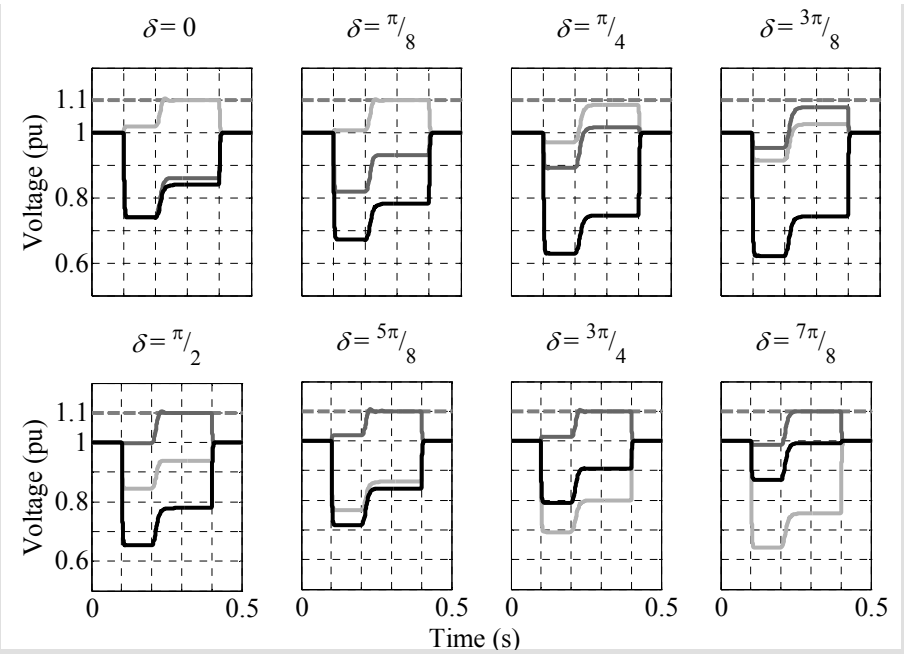

Fig. 8 Simulations for a set of voltage sags with common parameters V_p, V_n and varying sequence phase angle δ. Phase voltages: *a* in light grey, *b* in grey and *c* in black. Weak grid: L_g = 0.12 p.u., R/X=0.25.

Table 3 *Simulation results of sequence-currents and phase-current amplitudes*

δ	0	$\pi/8$	$\pi/4$	$3\pi/8$	$\pi/2$	$5\pi/8$	$3\pi/4$	$7\pi/8$
I_p	8.72	9.04	10.0	10.0	9.11	8.72	8.81	9.92
I_n	2.03	1.13	0.00	0.00	1.02	2.02	1.52	0.08
I_a	6.70	8.05	10.0	10.0	9.24	9.79	10.0	10.0
I_b	9.80	9.20	10.0	10.0	8.23	6.76	7.42	9.86
I_c	10.0	10.0	10.0	10.0	10.0	10.0	9.24	9.91

After examining the previous tests, it can be stated that the proposed controller has demonstrated its capability to meet the proposed control objectives in several grid scenarios.

6 Conclusions

This paper has presented an ancillary voltage support service for three-phase grid-connected low-power rating inverters operating under voltage sags. By adjusting the amount of the reactive current injected via positive and negative sequences, two different objectives can be fulfilled: first the injection of the maximum inverter current as reactive current, and second to raise the higher amplitude voltage to a predefined upper voltage boundary. Due to the growing number of DGS

present in the grid these objectives can favor a distributed voltage-support control, being this topic open for further research. A complete set of experimental results are reported in order to validate the effectiveness of the proposal.

7 References

[1] Blaabjerg, F., Teodorescu, R., Liserre, M., Timbus, A.V.: 'Overview of control and grid synchronization for distributed power generation systems', *IEEE Trans. Ind. Electron.*, 2006, **53**, (5), pp. 1398–1409

[2] Khadkikar, S., Chandra, A.: 'UPQC-S: A novel concept of simultaneous voltage sag/swell and load reactive power compensations utilizing series inverter of UPQC', *IEEE Trans. Power Electron.*, 2011, **26**, (9), pp. 2414–2425

[3] Bollen, M. H. J.: 'Understanding power quality problems: Voltage sags and interruptions', New York: IEEE Press, 2000.

[4] Ignatova, V., Granjon, P. and Bacha, S.: 'Space vector method for voltage dips and swells analysis', *IEEE Trans. on Power Delivery*, 2009, **24**, (4), pp. 2054–2061

[5] Djokic, S.Z., Milanovic, J.V.: 'Advanced voltage sag characterisation. Part I: Phase shift', *IEE Proc. Gener. Transm. Distrib.*, 2006, **153**, (4), pp. 423–430

[6] Cundeva, S., Neumann, R., Bollen, M., Kokolanski, Z., Vuletic, J., Krkoleva, A., Djokic, S., van Reusel, K, and Stockman K.: 'Immunity against voltage dips – Main recommendations to stakeholders of the CIGRE/CIRED/UIE Joint Working Group C4.110', 2011, pp. 555–563

[7] Djokic, S.Z., Milanovic, J.V. , Rowland, S.M.: 'Advanced voltage sag characterisation II: point on wave', *IET Gener. Transm. Distrib.*, 2007, **1**, (1), pp. 146–154

[8] IEC 61727–2004: 'Characteristics of the utility interface for photovoltaic systems', 2004

[9] Altin, M., Goksu, O., Teodorescu, R., Rodriguez, P., Jensen, B.-B., Helle, L.: 'Overview of recent grid codes for wind power integration', in *12th Int. Conf. on Optimization of Electrical and Electronic Equipment*, Brasov, Romania, May 2010, pp. 1152–1160

[10] Tsili, M., Papathanassiou, S.: 'A review of grid code technical requirements for wind farms', *IET Renew. Power Gen.*, 2009, **3**, (3), pp. 308–332

[11] Prodanovic, M., De Brabandere, K., Van den Keybus, J., Green, T., Driesen, J.: 'Harmonic and reactive power compensation as ancillary services in inverter-based distributed generation', *IET Gener. Transm. Distrib.*, 2007, **1**, (3), pp. 432–438

[12] Junyent-Ferre, A., Gomis-Bellmunt, O, Green, T.C., Soto-Sanchez, D.E.: 'Current control reference calculation issues for the operation of renewable source grid interface VSCs under unbalanced voltage sags', *IEEE Trans. Power Electron.*, 2011, **26**, (12), pp. 3744–3753

[13] Shang, L., Sun, D., Hu, J.: 'Sliding-mode-based direct power control of grid-connected voltage-sourced inverters under unbalanced network conditions', 2011, *IET Power Electron*., **4**, (5), pp. 570–579

[14] Wang, F., Duarte, J.L., Hendrix, M.A.M.: 'Pliant active and reactive power control for grid-interactive converters under unbalanced voltage dips', *IEEE Trans. Power Electron*., 2011, **26**, (5), pp. 1511–1521

[15] Eloy-Garcia, J., Arnaltes, S., Rodriguez-Amenedo, J.L.: 'Direct power control of voltage source inverters with unbalanced grid voltages', *IET Power Electron*., 2008, **1**, (3), pp. 395–407

[16] Miret, J., Castilla, M., Camacho, A., García de Vicuña, L., Matas, J.: 'Control scheme for photovoltaic three-phase inverters to minimize peak currents during unbalanced grid-voltage sags', *IEEE Trans. Power Electron*., 2012, **27**, (10), pp. 4262 - 4271

[17] Lee, C.-T., Hsu, C.-W., Cheng, P.-T.: 'A low-voltage ride-through technique for grid-connected converters of distributed energy resources', *IEEE Trans. Ind. Appl.*, 2011, **47**, (4), pp. 1821–1832

[18] Camacho, A., Castilla, M., Miret, J., Vasquez, J.C., Alarcon-Gallo, E.: 'Flexible voltage support control for three-phase distributed generation inverters under grid fault', *IEEE Trans.*

Ind. Electron., 2013, **60**, (4), pp.1429–1441

[19] Miret, J., Camacho, A., Castilla, M., Garcia de Vicuña, L., Matas, J.: 'Control scheme with voltage support capability for distributed generation inverters under voltage sags', *IEEE Trans. Power Electron.*, 2013, **28**, (11), 5252–5262

[20] Camacho, A., Castilla, M., Miret, J., Guzman, R., Borrell, A.: 'Reactive power control for distributed generation power plants to comply with voltage limits during grid faults', *IEEE Trans. Power Electron.*, 2014, **29**, (11), 2624–2634

[21] Castilla, M., Miret, J., Camacho, A., Matas, J., Garcia de Vicuna, L.: 'Voltage support control strategies for static synchronous compensators under unbalanced voltage sags', *IEEE Trans. Ind. Electron*, 2014, **61**, (2), pp. 808–820

[22] Matas, J., Castilla, M., Miret, J., Garcia de Vicuña, L., Guzman, R.: 'An adaptive pre-filtering method to improve the speed/accuracy trade-off of voltage sequence detection methods under adverse grid conditions', *IEEE Trans. Ind. Electron*, 2014, **61**, (5), pp. 2139–2151

[23] Asiminoaei, L., Teodorescu, R., Blaabjerg, F., Borup, U.: 'A digital controlled PV inverter with grid impedance estimation for ENS detection', *IEEE Trans. Power Electron.*, 2005, **20**, (11), pp. 1480–1490

[24] Zmood, D.N., Holmes, D.G., Bode, G.H.: 'Frequency-domain analysis of three-phase linear current regulators', *IEEE Trans. Ind. Applicat*., 2001, **37**, (2), pp. 601–610